

## COMPARISON OF SPEED-DENSITY MODELS IN THE AGE OF CONNECTED AND AUTOMATED VEHICLES

Amir Hossein Karbasi<sup>1</sup>, Behzad Bamdad Mehrabani<sup>2</sup>, Mario Cools<sup>3,4,5</sup>, Luca Sgambi<sup>2</sup>, and Mahmoud Saffarzadeh<sup>1</sup>

<sup>1</sup>*Department of Civil and Environmental Engineering, Tarbiat Modares University, Tehran, Iran*

<sup>2</sup>*Louvain Research Institute for Landscape, Architecture, Built Environment (LAB), Université Catholique de Louvain, Louvain-la-Neuve, Belgium*

<sup>3</sup>*Local Environment Management and Analysis (LEMA), UEE, University of Liege, Liege, Belgium*

<sup>4</sup>*Department of Informatics, Simulation and Modeling, KU Leuven Campus Brussel, Brussels, Belgium*

<sup>5</sup>*Faculty of Business Economics, Hasselt University, Diepenbeek, Belgium*

*Corresponding Author: Behzad Bamdad Mehrabani, behzad.bamdad@uclouvain.be*

**KEYWORDS:** operations, traffic simulation, automated/autonomous/connected vehicles, macroscopic traffic simulation

### ABSTRACT

Fundamental diagrams (FDs) present the relationship between flow, speed, and density, and give some valuable information about traffic features such as capacity, congested and uncongested situations, and so forth. On the other hand, high accuracy speed-density models can produce more efficient FDs. Although numerous speed-density models are presented in the literature, there are very few models for connected and autonomous vehicles (CAVs). One of the recent speed-density models that takes into account the penetration rate of CAVs is provided by Lu et al. However, the estimation power of this model has not been tested against other speed-density models, and it has not been applied to high-speed networks such as freeways. Thus, this paper made a comparison between the Lu speed-density model and a well-known speed-density model (Papageorgiou) in freeway and grid networks. Different CAV behaviors (aggressive, normal, and conservative) are evaluated in this comparison. The comparison has been made between two speed-density models using the mean absolute percentage error (MAPE) and a t-test. The MAPE and t-test results show that differences between the two speed-density models are not significant in two case studies and that Lu is a powerful speed-density model to estimate speed compared with a well-known speed-density model. For the sake of comparing the above-mentioned models, this paper investigates the impact of CAVs on capacity based on FDs. The results suggest that the magnitude of the impacts of CAVs on road capacity (capacity increment percentage) which are obtained from two speed-density models are very close to each other. Also, the extent to which CAVs affect road capacity is highly dependent on their behavior.

Fundamental diagrams (FDs), which represent the relationship between speed, density, and flow, play a vital role in traffic science and, with the help of FDs, some useful information such as density, speed, capacity, uncongested and congested situations, and so forth, can be obtained. For example, for the assessment of the quality of highway services, the speed-flow relationship can be used, and speed-density can indicate the change in traffic flow (1). Macroscopic traffic flow models perform better when a suitable speed-density relationship is chosen (2). Speed-density models are essential for analyzing traffic flow patterns.

For decades, many studies have tried to develop accurate and robust speed-density models, and these speed density models have different forms, such as linear, logarithmic, exponential, and so forth (3-10). Some of the earlier studies developed linear forms of speed-density models. That general form of the linear speed-density model was developed by May and Keller (5). This model has two shape parameters, and some other parameters include free-flow speed and jam density. Some other linear speed-density models are special forms of this model. For example, in models which are developed by Pipes and Drew, one of two shape parameters is equal to 1, and in the model developed by Greenshields et al., both shape parameters are equal to 1 (4, 6, 7). Another form of the speed-density model is logarithmic. A logarithmic speed-density model has been developed by Greenberg, and this model has two parameters: optimum speed and jam density. This model has no free-flow speed parameter, and it generates infinite speed (8). Other forms of speed-density models are exponential models, and these models fulfill flow-speed-density properties and represent empirical data robustly (2). For instance, Papageorgiou et al. developed an exponential speed-density model which has free-flow speed and critical density parameters, and this model has a shape parameter (3). In addition, there are some other exponential speed-density models, such as Drake et al. and Underwood, which are special forms of the Papageorgiou speed-density model (9, 10). However, these types of speed-density model did not pay attention to the effect of new technologies such as connected and autonomous vehicles (CAVs).

The rapid increase in the contribution of technologies in transportation provides the opportunity to reduce some of the traditional transportation problems. One of these technologies is CAVs, which are expected to positively affect various aspects of transportation, including capacity and safety (11-15). CAV technology has two main features: automation and connectivity. Automation refers to the ability to be driven by combinations of human and machine decision-making and control systems. The Society of Automotive Engineers (SAE) defines six levels of driving automation ranging from 0 (fully manual) to 5 (fully autonomous) (16). These levels of automation describe the sharing between humans and machines for controlling vehicles. This study investigates the impact of fully automated vehicles on traffic flow when automated vehicles are capable of performing all aspects of dynamic driving under any environmental and road conditions (16). The other feature (connectivity) can be considered as a feature that allows the vehicle to communicate with infrastructures (V2I), other vehicles (V2V), and pedestrians (V2P) (12).

CAVs (because of automation and connectivity features) have different behavior in relation to traffic operation than human-driven vehicles (HDVs). In other words, CAVs have different microscopic features based on the level of automation, connectivity, V2I, and V2V communication.

For example, fully connected and auto-mated vehicles with aggressive driving behavior can benefit from smaller headway and smaller distance between vehicles (12). Consequently, CAVs can affect FDs and some related components such as capacity, critical density, and congested and uncongested situations. However, none of the aforementioned speed-density models consider CAVs' effects, such as penetration rates of CAVs. To address this issue, Lu et al. developed a novel semiparametric speed-density model in which penetration rates of CAVs are considered, and they applied this speed-density model in urban networks (25). However, this model is not applied in high-speed networks such as freeways, and its estimation power has not been evaluated against other popular speed-density models, such as Papageorgiou et al.'s speed-density model (3). Moreover, Lu et al. only consider one type of driving behavior of CAVs, which is based on aggressive driving behavior (25). To fill these gaps, this paper aims to:

1. Compare the estimation power of Lu et al.'s speed-density model with a well-known speed-density model (the Papageorgiou speed-density model) (25).
2. Explore the power of Lu et al.'s speed-density model in freeways (25). The main motivation for this contribution is that the Lu model has only been applied to urban areas.
3. For comparison, investigate the impact of CAVs on the capacity of both freeways and urban areas using microsimulation and FDs. This paper first defines the driving behavior of HDVs and CAVs using microsimulation and determines the capacity using FDs. Because a majority of studies look at the effect of CAVs on capacity only based on one type of network, this paper investigates the impact of CAVs on the capacity of a low-speed network (a grid network) and a high-speed network (a freeway network) (13, 17-19).
4. Investigate the impact of CAVs on the capacity of freeways and urban roads based on three driving behavior of CAVs. This study defines CAV driving behavior based on aggressive, normal, and conservative driving behavior.

The remainder of the paper is organized as follows. In the next section, the study framework of this paper is presented. The section after that describes the results, and the final section presents the conclusions and suggestions for future studies.

## **STUDY FRAMEWORK**

To generate FDs and investigate the impact of CAVs on capacity, it is necessary to determine the differences between HDVs and CAVs based on microscopic driving behavior (car-following and lane-changing models).

Thus, this section has two parts: the first describes micro-simulations (the car-following model and the lane-changing model), and the second describes FDs (which are generated either directly from simulation data or by feeding simulation data into speed-density models). Figure 1 shows the framework of this study. Using microsimulation, the Krauss car-following model and the LC2013 lane-changing model (Simulation of Urban Mobility [SUMO] simulator lane-changing model) were applied to show HDV and CAV driving behavior. Car-following model and lane-changing model parameters were modified to demonstrate the difference between CAV and HDV driving behavior.

To generate FDs, two models have been applied by feeding simulation data into speed-density models: the Lu speed-density model and the Papageorgiou speed-density model (3, 25). By implementing these two speed-density models and the simulation data, FDs are specified, and thus their estimation power is compared. Moreover, the capacities of roads under different penetration rates of CAVs are calculated from FDs.

## MICROSIMULATION

There is, as yet, no practical use of CAVs in transportation networks. Therefore, simulation is a principal tool to determine how CAVs affect traffic flow in mixed traffic. Microscopic traffic simulation makes it possible to define the driving characteristics of both CAVs and HDVs. A variety of microsimulation software, such as VISSIM, PARAMICS, AIMSUN, and SUMO, are employed by researchers to analyze driving behavior. SUMO, the open-source microscopic traffic simulation software used in this study, allows us to modify driving behaviors and obtain desired information (20). This section describes the driving behavior of CAVs and HDVs utilizing the Krauss car-following model and the LC2013 lane-changing model (21, 22).

**Krauss Car-Following Model.** For analyzing the longitudinal movement of vehicles, the Krauss car-following model is employed, which describes the safe speed (21, 23). This car-following model is the default car-following model in the SUMO simulator. Unlike the Wiedemann car-following model in VISSIM software, which has an acceleration function for each traffic regime and is a psychophysiological model, the Krauss model is a space-continuous car-following model with an emphasis on maintaining the safe speed (24). In relation to parameter selection, longitudinal movement, acceleration, deceleration, and gap acceptance were taken into account (25). Thus, Krauss car-following parameters for mapping the longitudinal movement of HDVs and CAVs must be modified. Time headway, acceleration, and minimum gap for HDVs are based on the default value in the SUMO simulator, CAV parameters are taken from Atkins Ltd, and driver imperfection values ( $\sigma$ ) for HDVs and CAVs are taken from Lu et al. (12, 25, 26). These parameters are shown in Table 1. There are two important reasons for choosing CAV driving behavior from Atkins' study (12). First, this study suggests car-following values for urban and high-speed networks. Since this study investigates the impact of CAVs on the flow of both urban and freeway networks, car-following values based on Atkins's study are reasonable (12). Second, Atkins' study presents different driving behavior styles, from concrete to aggressive (12). On the other hand, one of our study's goals is to investigate the impact of CAVs on the capacity of transportation networks when the driving behavior of CAVs is based on three different driving behaviors—aggressive, normal, and conservative driving behavior. Thus, it can be realized that car-following model parameters, which are based on Atkins study, can show conservative, normal, and aggressive driving behavior (12). Atkins study presents nine levels of CAV driving behavior, from conservative (level = 1) to aggressive driving (level = 9) behavior (12). Thus, this study uses level 1 for conservative driving behavior, level 5 for normal driving behavior, and level 9 for aggressive driving behavior. It is reasonable that conservative driving behavior has higher headway, minimum gap, and lower acceleration, while normal and aggressive driving behavior have smaller headway, minimum gap, and higher acceleration.

**Lane-Changing.** It is important to note that one of the measures that show the vehicle's movement in microsimulation is lane-changing, which explains the lateral movement of vehicles (28). This study uses LC2013 lane-changing, a lane-changing model in the SUMO simulator (26). Three motivations for lane-changing in SUMO are illustrated in Figure 2 (strategic, cooperative, and tactical lane-changing). The first motivation is strategic lane-changing, which describes changing lanes when there is no connection between the current lane and the next edge on the route. Another motivation is cooperative lane-changing. There are times when vehicles perform lane-changing maneuvers solely to assist another vehicle in changing lanes, and this behavior is modeled in SUMO lane-changing named cooperative lane-changing. The vehicles are informed about being blocked followers by other vehicles in this model of lane changing. Thus, the ego vehicle may change lanes in either direction unless a strategic reason prevents vehicles from lane-changing to clear a space for the blocked vehicle (22). The third motivation is tactical lane-changing which allows the vehicle to change lanes when it follows a slower leader. Its most important parameter is modified to demonstrate how CAVs and HDVs behave based on the LC2013 lane-changing model.

To determine differences between CAVs and HDVs in lane-changing behavior, Mintsis et al. and Lücken et al. studies' results are used because these studies determined the differences between lane-changing behavior of HDVs and CAVs based on SUMO simulator lane-changing concepts (29, 30). The most important parameter of the lane-changing model for CAVs and HDVs is derived from these two studies. The study conducted by Mintsis et al. determined which parameter among several lane-changing model parameters would have the strongest influence on driving behavior from a lane-changing perspective (29). They found that the most effective parameter is *lcAssertive* which describes the "willingness to accept lower front and rear gaps on the target lane" (26). When *lcAssertive* values are higher, a vehicle's behavior toward shorter gaps is more aggressive and vehicles accept lower gaps for lane-changing, and when *lcAssertive* values are lower, the opposite is true and vehicles accept more gaps for lane-changing (29). Referring to the results of the Mintsis et al. study, the *lcAssertive* for HDVs is 1.3, while for CAVs, Lücken et al. showed that this parameter could vary from 0.6 to 0.8 (see Mintsis et al. and Lücken et al. for lane-changing value selection) (29, 30). In this research, the value of *lcAssertive* is set to 0.8 for aggressive driving behavior, 0.7 for normal driving behavior, and 0.6 for conservative driving behavior. All other parameters are set to SUMO's default values.

## FUNDAMENTAL DIAGRAM (FD)

FD is one of the key concepts in traffic flow theory and exhibits the relation between speed, density, and flow. FD determines the capacity (maximum flow rate) and critical density (density at capacity point). This capacity divides the traffic situation into two regimes: 1) traffic is in an uncongested state for densities lower than the critical density and 2) higher densities result in a congested state (31). Figure 3 shows an example of FDs.

The following equation describes the relationship between flow, density, and speed in FD:

$$Q_i(p_i) = V(p_i) \cdot p_i \quad (1)$$

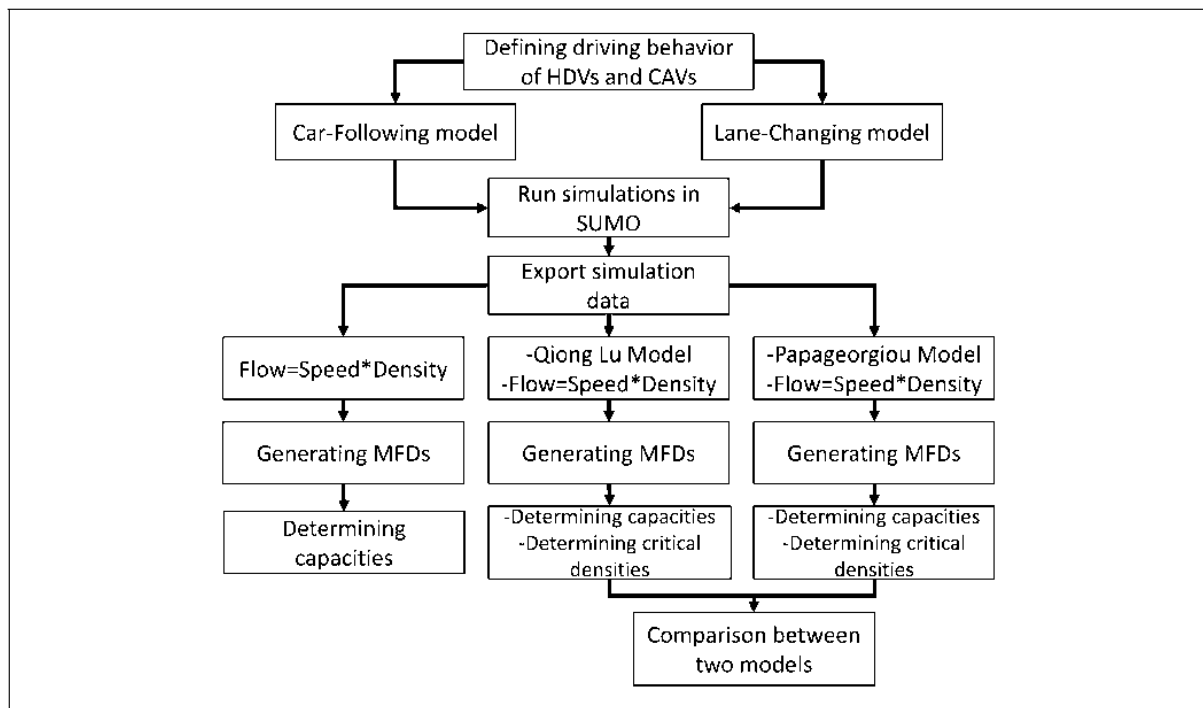
where

$Q_i(p_i)$  = flow (vehicles per hour [vph]),

$p_i$  = average density (vehicles per km), and

$V$  = speed (km/h).

**Figure 1.** Study framework.



Note: CAV = connected and autonomous vehicle; HDV = human-driven vehicle; MFD = macroscopic fundamental diagram.

**Table 1.** Human-Driven Vehicle (HDV) and Connected and Autonomous Vehicle (CAV) Car-Following Parameters

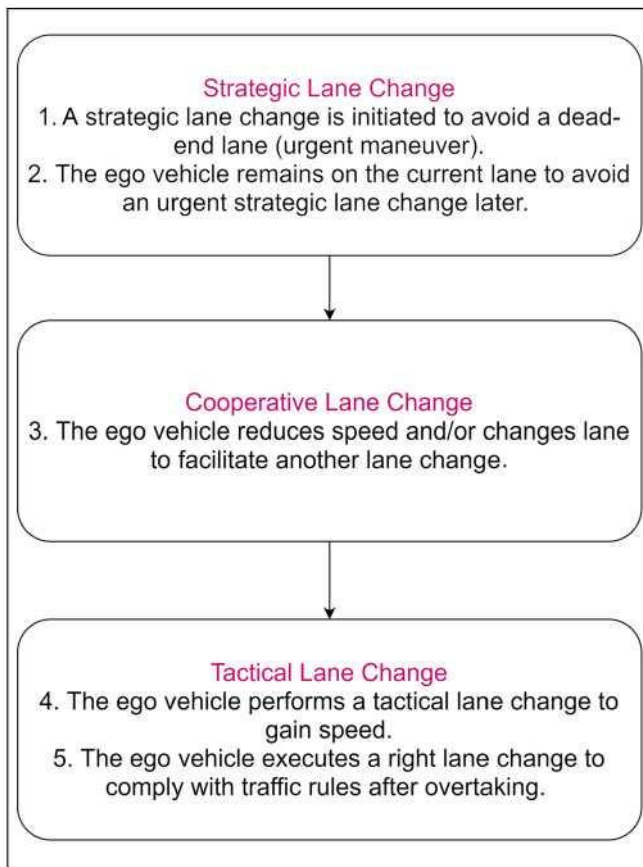
Vehicle type	tau	Mingap	Accel	Decel	Emergency decel	Sigma
HDV	1	2.5	2.6	4.5	8	0.5
CAV (aggressive)	0.5	0.5	3.9	4.5	8	0
CAV (normal)	0.9	1.5	3.5	4.5	8	0
CAV (conservative)	2.1	2.5	3.1	4.5	8	0

Note: Accel = the acceleration ability of vehicles of this type (m/s<sup>2</sup>); Decel = the deceleration ability of vehicles of this type (m/s<sup>2</sup>); Emergency decel = the maximum deceleration ability of vehicles of this type in case of emergency (m/s<sup>2</sup>); Mingap = minimum gap when standing (m); Sigma = the driver imperfection (0 to 1, 0 denotes perfect driving); tau = the driver's desired (minimum) time headway (s). In addition, to avoid collisions, deceleration and emergency deceleration are set equal for HDVs and CAVs (25). Also, sigma shows driver imperfection and can vary between 0 and 1; the 0 value shows perfect driving. In this study simulation environment, CAVs have perfect driving, and the value for HDVs is set to the simulation of urban mobility (SUMO) simulator default value. It should be pointed out that the road capacity offered by this study for HDVs may be different from the capacity offered by the Highway Capacity Manual (HCM) (2,300-2,400 vehicles per hour) when the speed limit is 100 km/h (27) as microscopic parameters are based on the SUMO simulator car-following and lane-changing model.

To generate FDs directly from simulation, some data, such as density and speed, are needed. Thus, the data were collected from the edge-based output in the SUMO simulator during simulations. The edge-based data includes some information about edges, such as link density, sample size, and average speed.

In the next two subsections, the Lu speed-density model and the Papageorgiou speed-density model that have been compared with each other in this study are discussed.

**Figure 2.** Hierarchy of lane-change logic (29).



Lu Speed-Density Model. Concerning the penetration rate of vehicle automation, Lu et al. developed a semiparametric speed-density model (25). This model calculates the speed as the following equation:

$$V(r, p) = a + s(p) + \beta \cdot r + \gamma \cdot rp \quad (2)$$

where

$a$  = average speed under free-flow conditions,

$s(p)$  = a non-parametric smooth function,

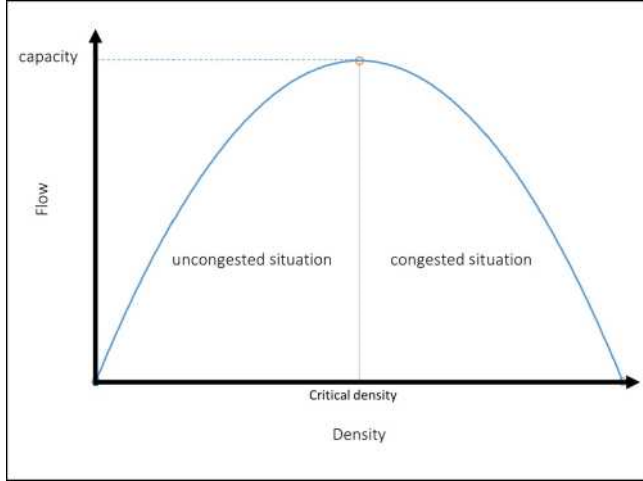
$\alpha$  = model parameter,

$\beta$  = model parameter,

$\gamma$  = model parameter, and

$r$  = vehicle automation penetration rate.

**Figure 3.** An example of fundamental diagrams (FDs).



In this model, vehicle automation penetration rates have been considered that affect free-flow average speed and the slope of the speed-density function. This model has two important features. First, it considers vehicle automation penetration rate, and, secondly, no assumptions need to be made about the baseline functional form of the speed-density curve. As a result, these features make this model powerful for estimation, and it is more straightforward to use for analysis of different penetration rates. In this model, semiparametric regression specification is estimated with a generalized additive model (GAM), originally a generalized linear model (GLM). The GLM describes a linear relationship between the unknown parameter and the mean of the dependent variable (25, 32). The form of GLM is:

$$g(\mu_{y|x}) = \beta_0 + \sum_{j=1}^p \beta_j x_j \quad (3)$$

where

$x_j$  = the independent variable,

$\beta_0$  = model parameter, and

$\beta_j$  = model parameter.

In GAM,  $\sum_{j=1}^p \beta_j x_j$  is replaced with  $\sum_{j=1}^p s_j(x_j)$ , where  $s_j(x_j)$  is a smooth function and is used to summarize the trend of a dependent variable  $Y$  as a function of several independent variables (see Liu for more information about GAM) (32).

Papageorgiou Speed-Density Model. The second speeddensity model is developed by Papageorgiou et al., as follows (3):

$$V(k) = v_f \exp \frac{-1}{c} \left( \frac{p}{p_m} \right)^c \quad (4)$$

where

$V$  = speed,



$v_f$  = a function of free-flow speed,

$p_m$  = critical density,

$p$  = density, and

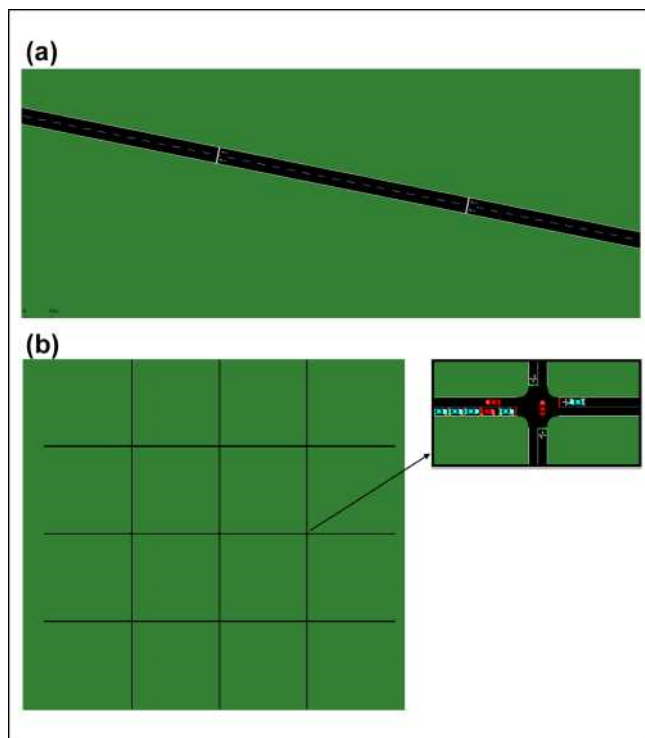
$c$  = the model shape parameter.

The difference between this model and the previous model is that the previous model considers the penetration rate of vehicle automation, but this model does not take into account the penetration rate of vehicle automation. To generate FDs, the speed-density models (Equations 2 and 4) should be substituted in Equation 1. The effect of CAVs on capacity is determined by the FDs.

## RESULTS

This section describes the results, which show the comparison between two speed-density models and determine the impact of CAVs on two case studies. Firstly, the case studies and their features are introduced. Then the modeling results are surveyed.

**Figure 4.** Case studies: (a) basic two-lane freeway and (b) grid network.



### CASE STUDIES

Two networks are simulated (shown in Figure 4). The first network is a basic two-lane freeway with a speed limit of 100 km/h and a length of 5 km. The second network is a grid network with 49 intersections with a speed limit of 50 km/h. All links of the grid network are bidirectional one-lane with a length of 400 m. All traffic lights have a fixed cycle time of 90 s. To simulate the uncongested condition in the basic freeway network, the demand has been increased from zero to the capacity

point. After this point, for creating congested conditions, variable speed signs (VSS) are used to create congestion (33). Ultimately, the demand declined to zero smoothly. This method is useful for both congested and uncongested situations and for generating FDs. The vehicles are routed randomly in the grid network by implementing Randomtrip.py (SUMO build-in tool) (26). As a result, the generated random trips are more flexible and homogenous in comparison with a demand model with fixed routes for the grid network (25). Moreover, in the case of a large network (such as the grid network in this study), the inserted vehicles are distributed randomly over the entire network, given a binomial distribution of inserted vehicles along each edge. This gives a reasonable approximation to the Poisson distribution (26).

## RESULTS OF FIRST CASE STUDY (BASIC FREEWAY)

In this section, comparison between two speed-density models is made, and the impact of CAVs on the capacity of the basic freeway (first case study) based on FDs is provided. To evaluate the impacts of CAVs, six scenarios were considered. In each scenario, the penetration rate of CAVs increased by 20% (starting by 0%). In the freeway network, for each scenario, data were obtained and aggregated based on 1 min time intervals (120 min in total). Ten iterations were considered for this case study.

**Lu and Papageorgiou Speed-Density Models.** GAM has been used to estimate the Lu speed-density model's coefficients. Table 2 shows a summary of coefficients estimations. In this table,  $R^2$ , the goodness of fit measure, is 0.89 for aggressive driving behavior, 0.91 for normal driving behavior, and 0.92 for conservative driving behavior, and these values demonstrate that this model is validated to estimate the relationship between speed, CAVs penetration rate, and density. To show that the null hypothesis is rejected and there is a relationship between speed and CAV penetration rate and density, the t-value should be far from zero, and the p-value should be small, which is the case for this model (25). Therefore, the model accurately describes the relationship between speed, penetration rate, and density of CAVs under different driving behavior. Table 2 shows some information about the impact of CAVs on average speed. Generally, parameter  $\alpha$  shows average speed under free-flow condition, which has a higher value for conservative driving behavior compared with aggressive and normal driving behavior (25). On the other hand,  $\beta$  and  $\gamma$  are coefficients that show the impact of the introduction of CAVs on average speed and speed-density function slope, respectively. Table 2 demonstrates that  $\beta$  is positive for aggressive and normal behavior and negative for conservative behavior, which means when CAVs have normal or aggressive driving behavior, they have a positive impact on average speed, and when CAVs have conservative driving behavior, they have a negative impact on average speed; the main reason is that HDVs behave more aggressively than CAVs with conservative behavior and the introduction of CAVs decreases average speed. On the other hand,  $\gamma$  shows how the introduction of CAVs influences the impact of increasing density on average speed so that, if  $\gamma$  is positive, CAVs can reduce the negative impact of increasing density on average speed (25). Table 2 shows that  $\gamma$  is positive for CAVs with aggressive and normal behavior and it can be realized that the negative impact of increasing density on average speed has reduced as a result of the introduction of CAVs with aggressive and normal behavior. Moreover,  $\gamma$  is negative for CAVs with conservative behavior,

which shows that CAVs with conservative driving behavior can strengthen the negative impact of increasing density on average speed. After the Lu speed-density model, this section reports the results obtained from the Papageorgiou speed-density model using an exponential curve (25). The statistical analysis of this model is reported in Table 3. Based on this table,  $R^2$  varies between 0.89 and 0.91, which indicates that this model can accurately estimate the relationship between density and speed.

The FDs, generated by both microsimulation data, the Lu speed-density model, and the Papageorgiou speed-density model, are illustrated in Figures 5 to 7. Figure 5 illustrates that the aggressive driving behavior of CAVs can increase the capacity of the freeway substantially. Figure 6 shows the impact of CAVs on the capacity of freeways based on normal driving behavior, and this figure demonstrates that CAVs can increase the capacity of the freeway network. Figure 7 shows the impact of CAVs on FDs based on conservative driving behavior. This figure illustrates that the conservative driving behavior of CAVs can reduce the capacity of the freeway network.

**Table 2.** Generalized Additive Model (GAM) Regression for the Basic Freeway (First Case Study)

Driving behavior	Coefficient	Estimate	Standard error	t-value	Pr(> t )	$R^2$
Aggressive	a	59.604	0.226	264.140	0.000	0.89
	$\beta$	0.022	0.007	3.367	0.001	
	$\gamma$	0.005	0.000	36.106	0.000	
	s(p)	na	na	na	0.000	
Normal	a	66.382	0.180	368.396	0.000	0.91
	$\beta$	0.043	0.006	7.307	0.000	
	$\gamma$	0.002	0.000	13.167	0.000	
	s(p)	na	na	na	0.000	
Conservative	a	77.757	0.169	459.989	0.000	0.92
	$\beta$	-0.070	0.007	-9.769	0.000	
	$\gamma$	-0.004	0.000	-17.985	0.000	
	S(p)	na	na	na	0.000	

Note: na = not applicable.

**Table 3.** Papageorgiou Speed-Density Model Regression Analysis for the Basic Freeway (First Case Study)

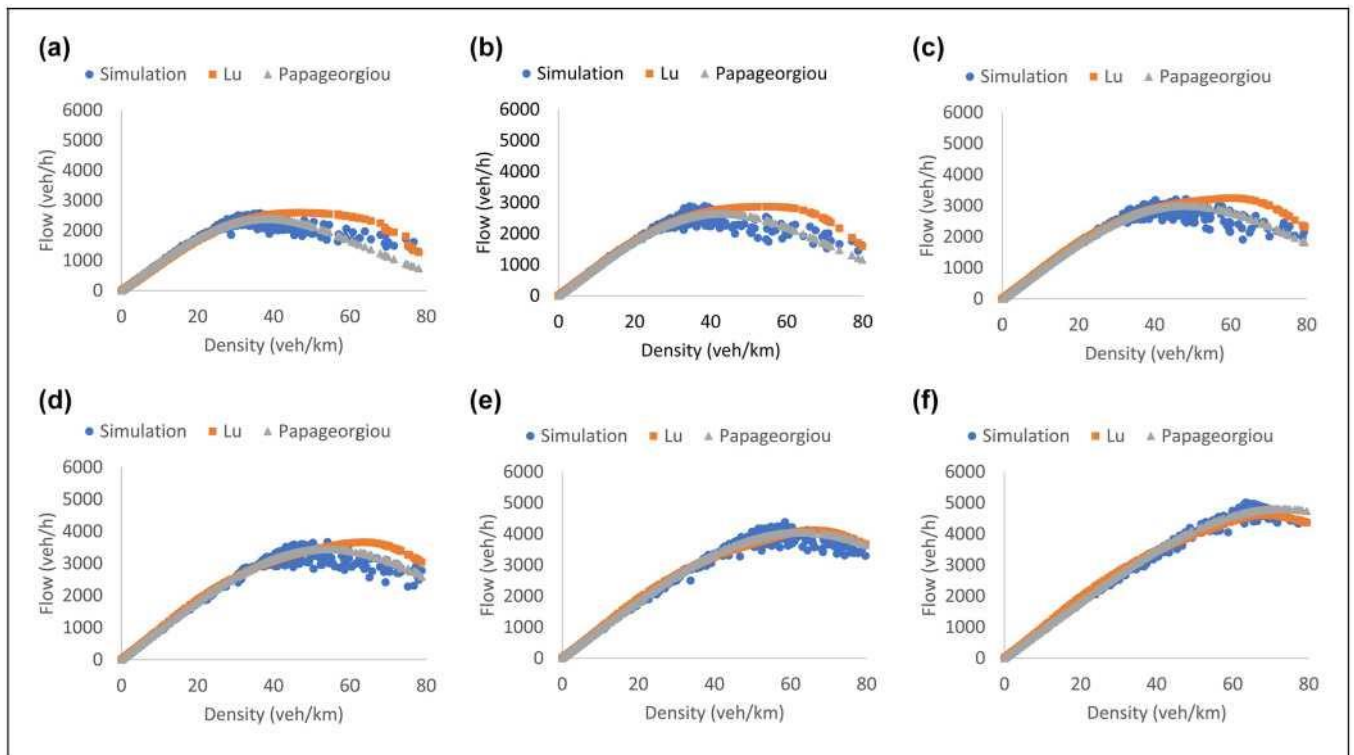
Driving behavior	PR	Estimation			Standard error			T-value			$R^2$
		$V_f$	$P_m$	c	$V_f$	$P_m$	c	$V_f$	$P_m$	c	
Aggressive	0	94.18	2.40	38.34	0.68	0.38	0.06	138.69	99.70	38.77	0.89
	20	93.78	2.40	42.78	0.66	0.46	0.06	141.18	92.56	37.98	0.89
	40	93.53	2.47	47.97	0.61	0.46	0.06	154.32	104.51	40.55	0.89
	60	93.02	2.61	54.36	0.55	0.46	0.06	169.36	118.89	43.17	0.9
	80	92.13	2.76	63.12	0.49	0.46	0.06	188.41	137.71	45.97	0.91
Normal	100	91.35	3.06	72.90	0.43	0.45	0.06	211.13	162.13	47.42	0.91
	0	94.18	38.34	2.40	0.68	0.38	0.06	138.69	99.70	38.77	0.89
	20	94.11	40.43	2.33	0.69	0.46	0.06	136.01	88.44	37.46	0.89
	40	93.90	42.52	2.41	0.65	0.43	0.06	144.37	99.10	39.51	0.9
	60	93.74	44.99	2.46	0.61	0.40	0.06	153.96	111.13	42.43	0.9
Conservative	80	93.17	47.38	2.51	0.58	0.39	0.06	161.39	120.66	44.09	0.91
	100	92.88	49.50	2.55	0.56	0.39	0.06	166.75	125.59	44.67	0.91
	0	94.18	2.40	38.34	0.68	0.38	0.06	138.69	99.70	38.77	0.89
	20	94.27	2.29	36.28	0.72	0.39	0.06	130.99	93.29	38.64	0.89
	40	94.20	2.23	34.07	0.73	0.34	0.06	129.26	99.50	40.48	0.89
	60	94.15	2.11	31.96	0.76	0.34	0.05	123.17	94.05	39.39	0.89
	80	94.24	2.03	29.73	0.80	0.33	0.05	117.75	89.40	38.45	0.9
	100	94.66	1.97	27.80	0.82	0.33	0.05	112.26	88.27	37.32	0.91

Note: PR = Penetration Rate.

*Published in : Transportation Research Record (2022)*  
*DOI: 10.1177/03611981221118531*  
*Status : Postprint (Author's version)*



**Figure 5.** FDs (speed-density relationship) based on aggressive driving behavior of CAVs (First case study): (a)  $PR=0$ , (b)  $PR=20$ , (c)  $PR=40$ , (d)  $PR=60$ , (e)  $PR=80$ , and (f)  $PR=100$ .

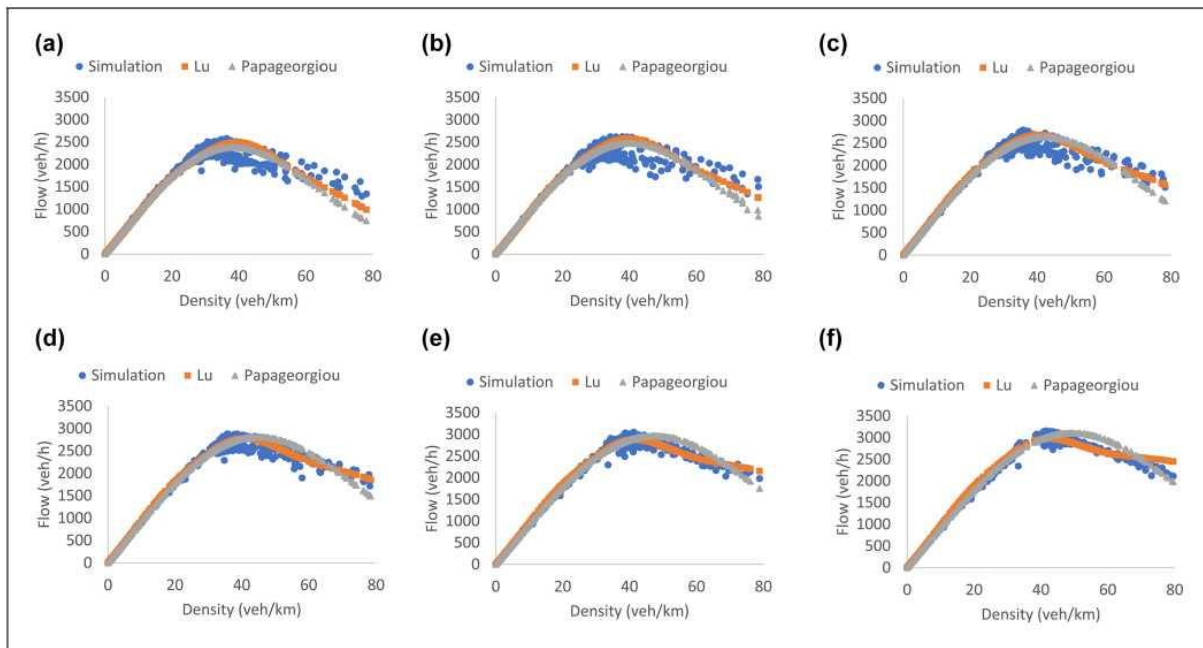


Note: PR = penetration rate.

In detail, Table 4 shows the impact of different driving behavior of CAVs on the capacity of freeways. This table confirms that aggressive driving behavior of CAVs increases the capacity of the freeway network by up to 101%, the normal behavior of CAVs can increase the capacity of freeway by up to 30%, and the conservative behavior of CAVs can reduce the capacity of the freeway by up to 34%.

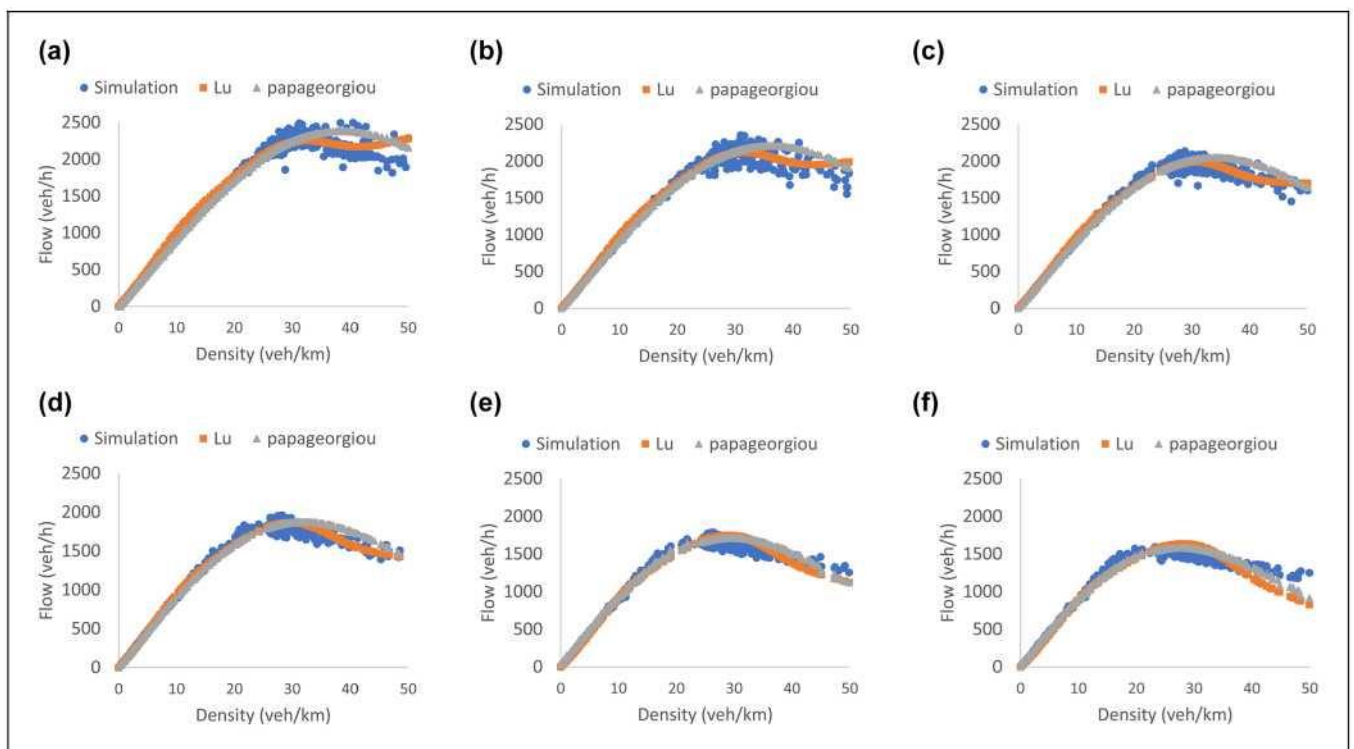
Generally, based on the driving behavior of CAVs, the impact of CAVs on the capacity of the freeway can vary between 234% and 101%. It is worth mentioning that this range of change is based on microscopic features discussed in the car-following and lane-changing section. Also, when the penetration rate is 0, the capacity is higher than HCM capacity. This is reasonable, because the driving behavior of HDVs is based on Krauss car-following parameters values; based on the different car-following models, a different capacity is obtained, and the value of capacity when  $PR = 0$  is near to the HCM value for a 100 km/h speed limit (2,300-2,400 vph) (27).

**Figure 6.** FDs (speed-density relationship) based on normal driving behavior of (CAVs) (first case study): (a) PR=0, (b) PR=20, (c) PR=40, (d) PR=60, (e) PR=80, (f) PR=100.



Note: PR = penetration rate.

**Figure 7.** FDs (flow-density relationship) based on conservative driving behavior of CAVs (first case study): (a) PR=0, (b) PR=20, (c) PR=40, (d) PR=60, (e) PR=80, and (f) PR=100.



Note: PR = penetration rate.

**Table 4.** Basic Freeway Capacity Change Based on Simulation, the Lu Model, and the Papageorgiou Model

Driving behavior	PR	Capacity (vphpl)			Percentage of capacity change compared with zero PR		
		Simulation	Lu	Papageorgiou	Simulation	Lu	Papageorgiou
Aggressive	0	2,576	2,592	2,381	na	na	na
	20	2,887	2,870	2,644	12.11	10.71	11.04
	40	3,216	3,241	2,994	24.85	25.00	25.74
	60	3,669	3,663	3,446	42.45	41.30	44.70
	80	4,386	4,123	4,046	70.30	59.03	69.90
Normal	100	5,013	4,616	4,801	94.63	78.07	101.61
	0	2,576	2,492	2,381	na	na	na
	20	2,624	2,586	2,477	1.89	3.75	4.02
	40	2,791	2,681	2,636	8.36	7.58	10.68
	60	2,880	2,779	2,810	11.80	11.51	18.01
Conservative	80	3,051	2,879	2,964	18.46	15.53	24.48
	100	3,158	2,982	3,106	22.61	19.66	30.44
	0	2,576	2,291	2,381	na	na	na
	20	2,353	2,119	2,208	-8.63	-7.50	-7.28
	40	2,136	1,990	2,049	-17.07	-13.14	-13.96
	60	1,961	1,866	1,874	-23.86	-18.54	-21.31
	80	1,788	1,748	1,713	-30.58	-23.69	-28.05
	100	1,592	1,636	1,583	-38.17	-28.60	-33.54

Note: vphpl = vehicles per hour per lane; PR = penetration rate; na = not applicable.

**Comparison of Speed-Density Models and Capacity Results.** Table 4 illustrates a comparison between capacities that are obtained from simulation (based on the relationship between speed, density, and flow), the Lu speed-density model, and the Papageorgiou speed-density model (25). This table shows that differences between capacities are not significant. To prove that the differences between capacities are not significant, a t-test is used. T-tests are done between simulation and Lu capacities, Lu and Papageorgiou capacities, and simulation and Papageorgiou capacities. P-values show that the differences between the two models are not significant. To compare the performance of the two speed-density models, the mean absolute percentage error (MAPE) and t- test for both models per penetration rate are calculated (Table 5). MAPE is calculated as following Equation 5:

$$MAPE = \left( \frac{1}{N} \sum_{t=1}^N \left| \frac{S_t - E_t}{S_t} \right| \right) \times 100 \quad (5)$$

where

$N$  = the number of observed speeds or flows,

$S_t$  = the simulation value, and

$E_t$  = the speed-density model value.

Generally speaking, based on MAPE, the Papageorgiou model shows better performance in estimating speed compared with the Lu model. However, the difference between the two models' speeds and two models' flows values is neglectable. To prove that the differences between the two models' speeds and flows values are not significant, the t-test is used. Based on the p-values of the t-test, which are shown in Table 5, all values are much higher than 0.05, which shows that differences between the two models' speeds and flow values are not significant. Therefore, it can be concluded that, although there are some differences between the MAPE value of the two speed-

density models, the Lu model shows an acceptable performance in comparison with the well-known Papageorgiou model.

**Table 5.** Mean Absolute Percentage Error (MAPE) Results of Lu and Papageorgiou Speed-Density Models

Driving behavior	MAPE speed		P-value
	Lu speed-density model	Papageorgiou speed-density model	
Aggressive	9.06	5.06	0.27
Normal	5.02	5.02	0.34
Conservative	3.91	3.53	0.47

**Table 6.** Generalized Additive Model (GAM) Regression for Grid Network (Second Case Study)

Driving behavior	Coefficient	Estimate	Standard error	t-value	Pr(> t )	R <sup>2</sup>
Aggressive	a	29.16	0.086	338.11	0.000	0.98
	$\beta$	0.032	0.002	14.27	0.000	
	$\gamma$	0.001	0.000	9.99	0.000	
	s(p)	na	na	na	0.000	
Normal	a	28.008	0.067	420.74	0.000	0.99
	$\beta$	0.023	0.002	13.77	0.000	
	$\gamma$	0.000	0.000	3.70	0.000	
	s(p)	na	na	na	0.000	
Conservative	a	26.570	0.065	410.108	0.000	0.97
	$\beta$	20.002	0.0002	22.955	0.033	
	$\gamma$	0.000	0.000	24.730	0.000	
	s(p)	na	na	na	0.000	

Note: na = not applicable.

## RESULTS OF SECOND CASE STUDY (GRID NETWORK)

In this section, the comparison between the two speed-density models is made, and the impact of CAVs on the capacity of the grid network is evaluated. Similar to the first case study, six scenarios have been defined. In each scenario, the penetration rate of CAVs increased by 20%. Data were obtained and aggregated in the grid network for each scenario based on 1 min time intervals (45 min in total). Moreover, each simulation is repeated ten times (ten iterations).

**Lu and Papageorgiou Speed-Density Models.** To survey the Lu speed-density model statistically, Table 6 shows a summary of the estimation of coefficients. In this model, all of the R<sup>2</sup> are over 0.95, which indicates this model can explain the relationship between speed, CAVs penetration rate, and density with high accuracy.

Table 6 illustrates that in aggressive driving behavior of CAVs, parameter a has a higher value than in conservative and normal driving behavior. In addition, parameter  $\beta$  is positive for aggressive and normal behavior and is negative for conservative behavior, which means that CAVs with normal and aggressive driving behavior have a positive impact on average speed and CAVs with conservative driving behavior have a negative impact on average speed. Moreover, Table 6 shows that the parameter  $\gamma$  is positive for aggressive and zero for conservative behavior and normal behavior. As mentioned before,  $\gamma$  shows whether CAVs can change the impact of increasing density on average speed. Consequently, CAVs with aggressive driving behavior can decrease the negative impacts of increasing density on speed. However, CAVs with normal and conservative driving



behavior cannot mitigate the negative effect of density increment on speed. Table 7 provides the results of the Papageorgiou model's statistical analysis, which demonstrates that speed can be accurately estimated using this model ( $R^2$  varies between 0.96 and 0.99, all t-values are far from zero, and all p-values are equal to zero).

To illustrate the impact of CAVs on capacity, FDs are used; however, because there are a lot of routes and flows in the grid network, the average flow, speed, and density of the whole network are used to generate FDs. Thus, macroscopic fundamental diagrams (MFDs) are used to explore the impact of CAVs on the capacity of the grid network. The MFDs, generated by microsimulation data, the Lu speed-density model, and the Papageorgiou speed-density model, are illustrated in Figures 8 to 10. Figure 8 illustrates that the aggressive driving behavior of CAVs increases the capacity of the grid network. Figure 9 demonstrates the impact of CAVs on the capacity of the grid network based on normal driving behavior, and this figure shows that CAVs increase the capacity of the grid network. Finally, Figure 10 shows the impact of CAVs on MFDs based on conservative driving behavior. This figure illustrates that the conservative driving behavior of CAVs decreases the capacity of the grid network.

In detail, Table 8 illustrates the impact of different styles of driving behavior of CAVs on the capacity of the grid network. This table shows that the aggressive driving behavior of CAVs increases the capacity of the grid network by up to 18%, the normal behavior of CAVs increases the capacity of the grid network by up to 43%, and the conservative behavior of CAVs decreases the capacity of the grid network by up to 14%. Generally, based on the driving behavior of CAVs, the impact of CAVs on the grid network capacity can vary between -14% and 43%. It is worth mentioning that this range of change is based on microscopic features discussed in the car-following and lane-changing sections.

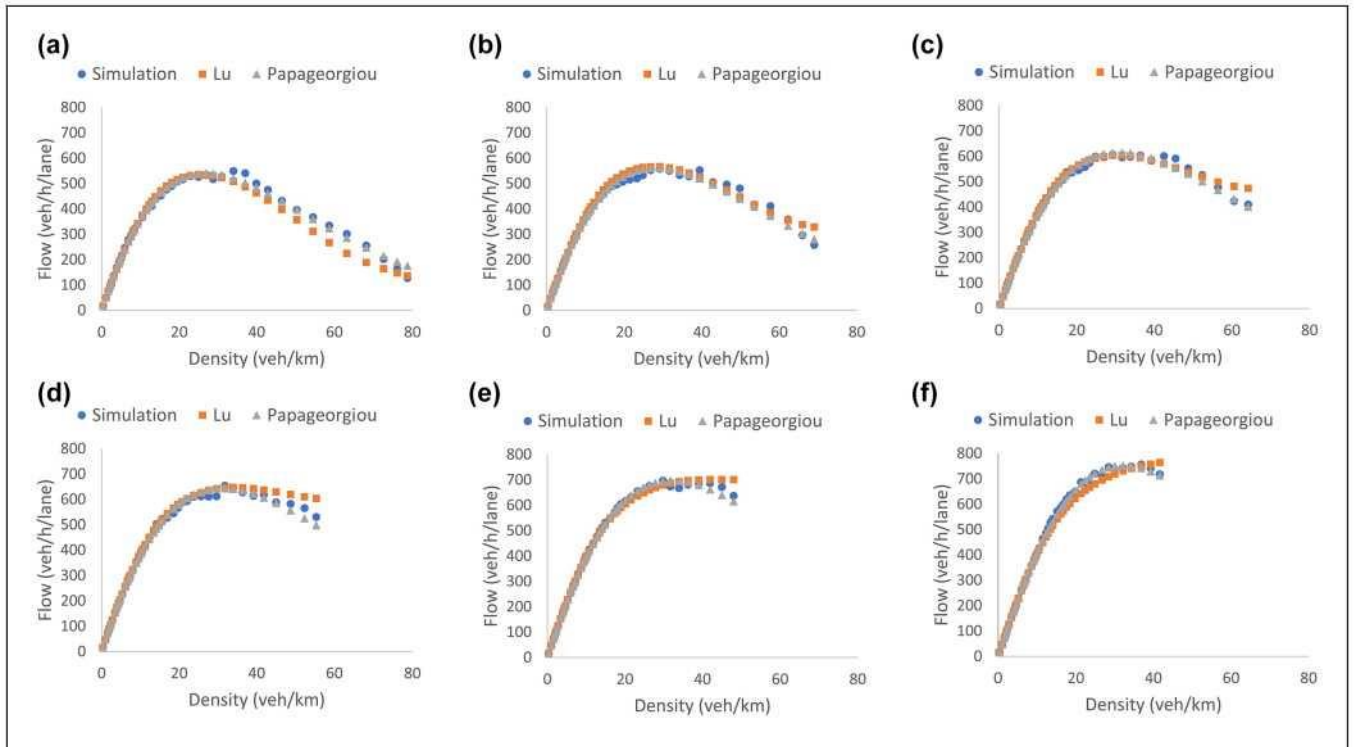
Comparison of Speed-Density Models and Capacity Results. Table 8 compares the capacities obtained from simulation, the Lu speed-density model, and the Papageorgiou speed-density model. As shown in this table, the three approaches give similar results for evaluating the capacity of the grid network. Based on MAPE results, the Papageorgiou model shows superior performance in three styles of driving behavior of CAVs. Based on the results of the t-test (Table 9), it can be claimed that there is no significant difference between the two models. Therefore, it can be concluded that the Lu model shows powerful performance compared with the well-known Papageorgiou model.

**Table 7.** Papageorgiou Speed-Density Model Regression Analysis for Grid Network (Second Case Study)

Driving behavior	PR	Estimation			Standard error			T-value			R <sup>2</sup>
		V <sub>f</sub>	P <sub>m</sub>	c	V <sub>f</sub>	P <sub>m</sub>	c	V <sub>f</sub>	P <sub>m</sub>	c	
Aggressive	0	46.33	26.84	1.20	0.27	0.30	0.02	174.30	89.43	62.01	0.99
	20	46.41	28.18	1.18	0.27	0.35	0.02	171.08	80.32	58.40	0.99
	40	46.64	30.84	1.18	0.24	0.38	0.02	195.65	82.04	62.66	0.98
	60	46.70	31.20	1.22	0.25	0.44	0.02	190.30	70.55	54.34	0.97
	80	46.61	32.15	1.31	0.19	0.42	0.02	244.34	75.77	58.90	0.97
Normal	100	46.26	32.22	1.46	0.22	0.60	0.04	209.00	53.98	40.40	0.99
	0	46.33	26.84	1.20	0.27	0.30	0.02	174.30	89.43	62.01	0.99
	20	46.60	26.28	1.19	0.24	0.27	0.02	195.68	96.98	68.97	0.98
	40	46.41	26.44	1.27	0.19	0.22	0.02	243.86	122.71	80.97	0.97
	60	47.03	28.79	1.18	0.24	0.32	0.02	199.68	88.76	65.89	0.98
Conservative	80	47.30	29.91	1.19	0.26	0.40	0.02	178.81	75.69	56.60	0.97
	100	47.36	30.35	1.23	0.28	0.46	0.02	172.01	65.41	49.64	0.96
	0	46.33	26.84	1.20	0.27	0.30	0.02	174.30	89.43	62.01	0.97
	20	47.15	27.33	1.11	0.36	0.43	0.02	130.19	63.87	48.92	0.98
	40	47.42	27.43	1.10	0.32	0.37	0.02	148.61	73.64	56.61	0.98
	60	47.61	26.57	1.13	0.34	0.37	0.02	139.27	71.95	53.12	0.97
	80	48.35	25.21	1.10	0.37	0.37	0.02	131.44	67.90	51.26	0.96
	100	48.66	24.50	1.11	0.38	0.37	0.02	128.46	66.95	50.02	0.98

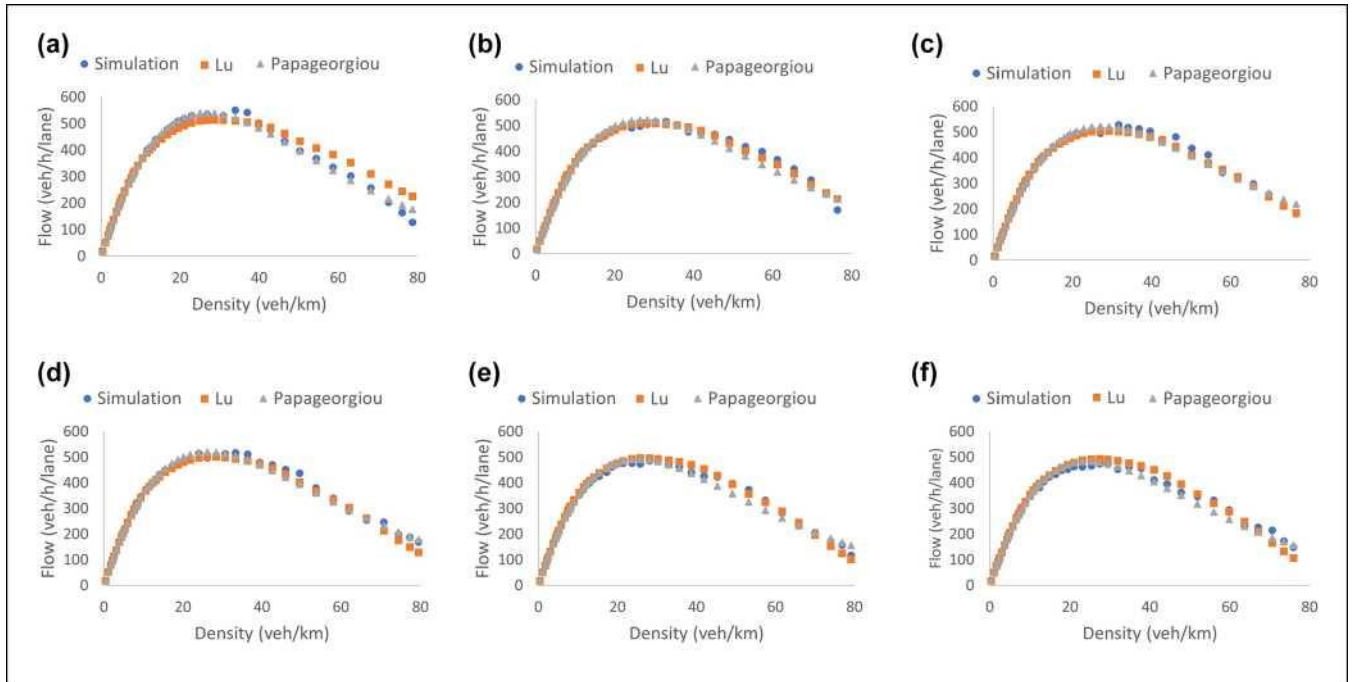
Note: PR = penetration rate.

**Figure 8.** MFDs (speed-density relationship) based on aggressive driving behavior of CAVs (second case study): (a) PR=0, (b) PR=20, (c) PR=40, (d) PR=60, (e) PR=80, and (f) PR=100.



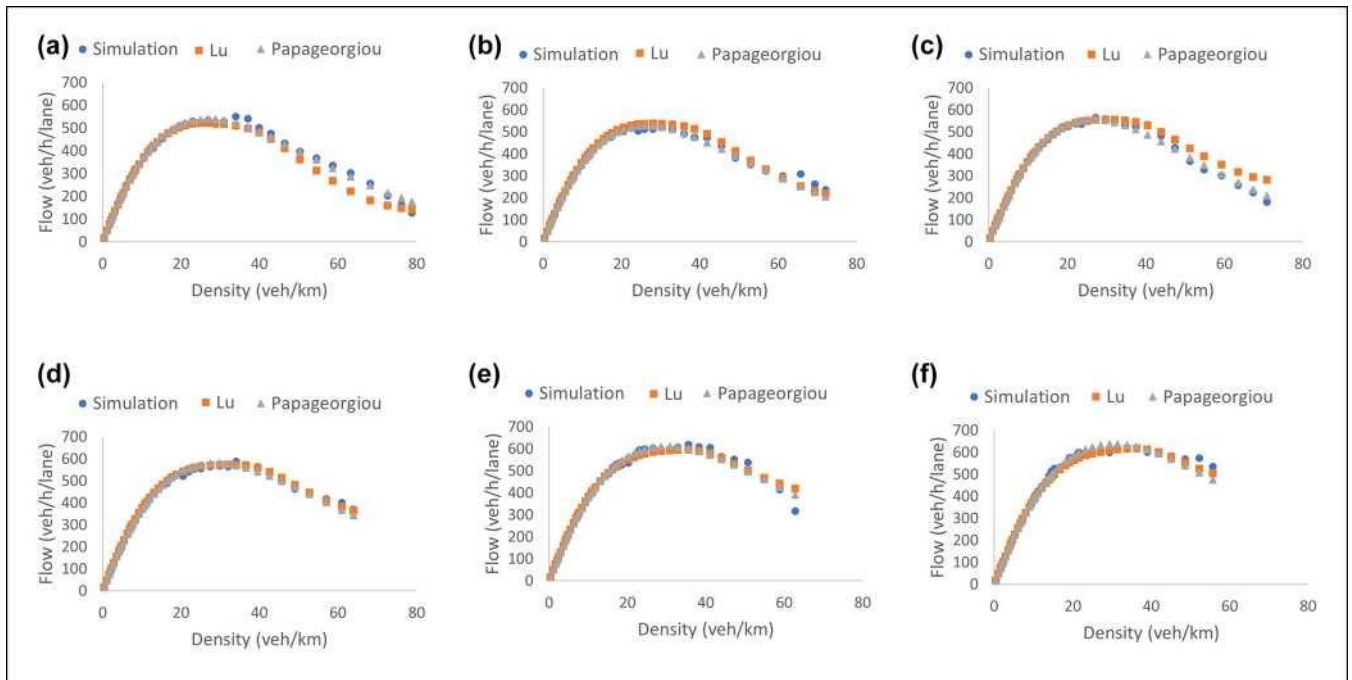
Note: PR = penetration rate.

**Figure 9.** MFDs (speed-density relationship) based on normal driving behavior of CAVs (second case study): (a)  $PR=0$ , (b)  $PR=20$ , (c)  $PR=40$ , (d)  $PR=60$ , (e)  $PR=80$ , and (f)  $PR=100$ .



Note: PR = penetration rate.

**Figure 10.** MFDs (flow-density relationship) based on conservative driving behavior of CAVs (second case study): (a)  $PR=0$ , (b)  $PR=20$ , (c)  $PR=40$ , (d)  $PR=60$ , (e)  $PR=80$ , and (f)  $PR=100$ .



Note: PR = penetration rate.

**Table 8.** Grid Network Capacity Change Based on Simulation, the Lu Model, and the Papageorgiou Model

Driving behavior	PR	Capacity (vphpl)			Percentage of capacity change compared with zero PR		
		Simulation	Lu	Papageorgiou	Simulation	Lu	Papageorgiou
Aggressive	0	550	534	540	na	na	na
	20	558	567	561	1.54	6.02	3.80
	40	607	604	615	10.44	13.00	13.74
	60	654	647	644	18.95	21.11	19.11
	80	697	701	697	26.83	31.16	29.04
	100	757	764	752	37.69	42.97	39.20
Normal	0	550	522	540	na	na	na
	20	520	538	528	-5.47	3.06	-2.38
	40	564	555	557	2.57	6.36	3.08
	60	588	574	579	6.95	10.06	7.22
	80	620	595	611	12.69	14.06	13.09
	100	617	618	638	12.14	18.36	18.08
Conservative	0	550	514	540	na	na	na
	20	515	509	522	-6.35	-0.87	-3.39
	40	528	505	522	-4.02	-1.72	-3.36
	60	516	500	520	-6.13	-2.59	-3.68
	80	485	496	492	-11.76	-3.38	-8.98
	100	473	492	484	-13.90	-4.14	-10.51

Note: PR = penetration rate; vphpl = vehicles per hour per lane; na = not applicable.

**Table 9.** Mean Absolute Percentage Error (MAPE) Results of the Lu and Papageorgiou Speed-Density Models

Driving behavior	MAPE speed		P-value
	Lu speed-density model	Papageorgiou speed-density model	
Aggressive	3.07	2.27	0.44
Normal	2.83	1.91	0.42
Conservative	3.71	3.25	0.49

## CONCLUSION

In this paper, a comparison between a novel speed density model which considers CAV penetration rates and the Papageorgiou speed-density model has been made, and the impact of CAVs based on three different driving behaviors on the capacity of transportation net-works has been investigated. On the one hand, many different speed-density models did not consider the effect of CAVs in their models, and, on the other hand, the estimation of the new speed-density model, developed by Lu et al., which considers the CAV penetration rate, is not compared with other speed-density models to realize its estimation power (25). In addition, the Lu speed-density model is not tested for high-speed networks such as basic freeways (25). Moreover, Lu et al. only consider the aggressive driving behavior of CAVs (25). Therefore, to fill these gaps, in this paper, the Lu speed-density model is tested for the basic freeway and grid networks, and this model is compared with the Papageorgiou speed-density model (3, 25). In addition, this study defines the driving behavior of CAVs based on aggressive, normal, and conservative driving behavior.

The microsimulation is carried out by implementing the SUMO simulator. To show the difference in driving behavior between CAVs and HDVs, Krauss car-following parameters and LC2013 lane-changing model parameters are modified. To investigate the impact of CAVs on the capacity of

roads, six scenarios are considered. In every scenario, the penetration rate of CAVs increases by 20% (starting at 0%). Then, the microsimulation data are fed into two speed-density models, namely the Lu and Papageorgiou models, to generate FDs. The FDs extracted directly from simulation, the FDs generated by simulation data, and the two speed-density models are compared.

A comparison is performed between the two speed-density models, which reveals the better performance of the Papageorgiou model based on MAPE in the basic freeway network. However, the t-test shows that the difference between the Papageorgiou and Lu models is small. It can be realized that Lu is also a powerful model to estimate speed in the basic freeway network. In the grid network, the comparison results between the two speed-density models show that the Papageorgiou model performs better. However, the t-test indicates that the Papageorgiou and Lu models have small differences in speed estimation. It is concluded that the Lu model can estimate the speed with high accuracy compared with the Papageorgiou speed-density model, which is a well-known speed-density model in the grid network. Also, the results confirmed that capacities obtained from the two models are close to each other, and differences between capacities are not significant. Moreover, the results confirm that CAVs have the ability to increase the capacity of basic freeways by up to 101% based on aggressive driving behavior, and CAVs can reduce the capacity of freeway by up to 34% based on conservative driving behavior. Also, they can increase the capacity of the grid network by up to 43% when CAV movements are based on aggressive driving behavior, and CAVs can decrease the capacity of the grid network by up to 14% based on conservative driving behavior. It should be noted that the results of the impact of CAVs on capacity are based on aggressive, conservative, and normal driving behavior and microscopic features, which have been discussed in Krauss car-following model section and lane-changing section. If the behavior of CAVs with regard to lane-changing and car-following behavior varies, the results will change.

Future research should pay attention to comparing the Lu model with other speed-density models using real data. Also, future studies should investigate the lane-changing model more deeply and modify more lane-changing parameters. Other car-following models like the intelligent driver model (IDM) and cooperative adaptive cruise control (CACC) can also be tested. Moreover, it can be more realistic to calibrate Krauss car-following model parameters for HDV driving behavior based on real traffic data. Given that the Lu model is a novel model, future work can focus on improving this model. Also, future studies should investigate the impact of CAVs on more complex networks such as weaving and merge freeway networks. Based on the SUMO simulator setting, this study did not explore the effect of reaction time on driving behavior performance; thus, future studies can investigate the impact of reaction time on the behavior of HDVs and CAVs.

## **AUTHOR CONTRIBUTIONS**

The authors confirm contribution to the paper as follows: study conception and design: A. Karbasi, B. Bamdad Mehrabani, L. Sgambi, M. Saffarzadeh; data collection: A. Karbasi, B. Bamdad Mehrabani; analysis and interpretation of results: A. Karbasi, B. Bamdad Mehrabani, M. Cools., L.

Sgambi; draft manuscript preparation: A. Karbasi, B. Bamdad Mehrabani, M. Cools. All authors reviewed the results and approved the final version of the manuscript.

## **DECLARATION OF CONFLICTING INTERESTS**

The author(s) declared no potential conflicts of interest with respect to the research, authorship, and/or publication of this article.

## **FUNDING**

The authors disclosed receipt of the following financial support for the research, authorship, and/or publication of this article: The corresponding author was supported by the Université catholique de Louvain under the “Fonds Spéciaux de Recherche” program.

## **ORCID IDS**

Behzad Bamdad Mehrabani : <https://orcid.org/0000-0001-8585-7879>

Mario Cools : <https://orcid.org/0000-0003-3098-2693>

## References

1. Yu, C., J. Zhang, D. Yao, R. Zhang, and H. Jin. Speed-Density Model of Interrupted Traffic Flow Based on Coil Data. *Mobile Information Systems*, Vol. 2016, 2016, pp. 1-12.
2. Gaddam, H. K., and K. R. Rao. Speed-Density Functional Relationship for Heterogeneous Traffic Data: A Statistical and Theoretical Investigation. *Journal of Modern Transportation*, Vol. 27, No. 1, 2019, pp. 61-74.
3. Papageorgiou, M., J.-M. Blosseville, and H. Hadj-Salem. Macroscopic Modelling of Traffic Flow on the Boulevard Peripherique in Paris. *Transportation Research Part B: Methodological*, Vol. 23, No. 1, 1989, pp. 29-47.
4. Greenshields, B., J. Bibbins, W. Channing, and H. Miller. A Study of Traffic Capacity. Proc., Highway Research Board, Washington, D.C., National Research Council (USA), Highway Research Board, 1935.
5. May, A. D., and H. E. Keller. Non-Integer Car-Following Models. *Highway Research Record*, Vol. 199, No. 1, 1967, pp. 19-32.
6. Drew, D. R. *Traffic Flow Theory and Control*. McGraw-Hill, New York, NY, 1968.
7. Pipes, L. A. Car-Following Models and the Fundamental Diagram of Road Traffic. *Transportation Research*, Vol. 1, 1967, pp. 21-29.
8. Greenberg, H. An Analysis of Traffic Flow. *Operations Research*, Vol. 7, No. 1, 1959, pp. 79-85.
9. Drake, J., J. Schofer, and A. May. A Statistical Analysis of Speed Density Hypotheses. *Highway Research Record*, Vol. 154, 1967, pp. 53-87.
10. Underwood, R. T. Speed, Volume and Density Relationships. In *Quality and Theory of Traffic Flow*, Bureau of Highway Traffic, Yale University, New Haven, 1961, pp. 141-187.
11. Mehrabani, B. B., L. Sgambi, E. Garavaglia, and N. Madani. Modeling Methods for the Assessment of the Ecological Impacts of Road Maintenance Sites. In *Environmental Sustainability and Economy* (P. Singh, P. Verma, D. Perrotti, and K. K. Srivastava, eds.), Elsevier, 2021, pp. 171-193.
12. Atkins Ltd. *Research on the Impacts of Connected and Autonomous Vehicles (CAVs) on Traffic Flow*. Department of Transport, London, 2016.
13. Liu, P., and W. Fan. Exploring the Impact of Connected and Autonomous Vehicles on Freeway Capacity Using a Revised Intelligent Driver Model. *Transportation Planning and Technology*, Vol. 43, No. 3, 2020, pp. 279-292.
14. Viridi, N., H. Grzybowska, S. T. Waller, and V. Dixit. A Safety Assessment of Mixed Fleets with Connected and Autonomous Vehicles Using the Surrogate Safety Assessment Module. *Accident Analysis & Prevention*, Vol. 131, 2019, pp. 95-111.
15. Karbasi, A., and S. O'Hern. Investigating the Impact of Connected and Automated Vehicles on Signalized and Unsignalized Intersections Safety in Mixed Traffic. *Future Transportation*, Vol. 2, No. 1, 2022, pp. 24-40.
16. SAE International. *Taxonomy and Definitions for Terms Related to Driving Automation Systems for On-Road Motor Vehicles*, SAE International, Warrendale, PA, 2018.

17. Zhong, Z., E. E. Lee, M. Nejad, and J. Lee. Influence of CAV Clustering Strategies on Mixed Traffic Flow Characteristics: An Analysis of Vehicle Trajectory Data. *Transportation Research Part C: Emerging Technologies*, Vol. 115, 2020, p. 102611.
18. Talebpour, A., and H. S. Mahmassani. Influence of Connected and Autonomous Vehicles on Traffic Flow Stability and Throughput. *Transportation Research Part C: Emerging Technologies*, Vol. 71, 2016, pp. 143-163.
19. Ghiasi, A., O. Hussain, Z. S. Qian, and X. Li. A Mixed Traffic Capacity Analysis and Lane Management Model for Connected Automated Vehicles: A Markov Chain Method. *Transportation Research Part B: Methodological*, Vol. 106, 2017, pp. 266-292.
20. Lopez, P. A., M. Behrisch, L. Bieker-Walz, J. Erdmann, Y.-P. Flotterod, R. Hilbrich, L. Lucken, J. Rummel, P. Wagner, and E. Wießner. Microscopic Traffic Simulation Using Sumo. Proc., 2018 21st International Conference on Intelligent Transportation Systems (ITSC), Maui, HI, IEEE, New York, 2018, pp. 2575-2582.
21. Krauss, S. Microscopic Modeling of Traffic Flow: Investigation of Collision Free Vehicle Dynamics. PhD thesis. Universität zu Köln, 1998.
22. Erdmann, J. SUMO's Lane-Changing Model. In *Modeling Mobility with Open Data* (M. Behrisch, and M. Weber, eds.), Springer, Cham, 2015, pp. 105-123.
23. Song, J., Y. Wu, Z. Xu, and X. Lin. Research on Car-Following Model Based on SUMO. Proc., The 7th IEEE/International Conference on Advanced Infocomm Technology, Fuzhou, China, IEEE, New York, 2014, pp. 47-55.
24. Wiedemann, R. Simulation Des Straßenverkehrsflusses. Institut für Verkehrswesen der Universität Karlsruhe, Heft 8, Karlsruhe, Germany, 1974.
25. Lu, Q., T. Tettamanti, D. Horcher, and I. Varga. The Impact of Autonomous Vehicles on Urban Traffic Network Capacity: An Experimental Analysis by Microscopic Traffic Simulation. *Transportation Letters*, Vol. 12, No. 8, 2020, pp. 540-549.
26. SUMO. SUMO User Documentation. <https://sumo.dlr.de/docs/index.html>.
27. Highway Capacity Manual. A Guide for Multimodal Mobility Analysis. Transportation Research Board, Washington, D.C., 2016.
28. Mullakkal-Babu, F. A., M. Wang, B. van Arem, and R. Happee. Empirics and Models of Fragmented Lane Changes. *IEEE Open Journal of Intelligent Transportation Systems*, Vol. 1, 2020, pp. 187-200.
29. Mintsis, E., D. Koutras, K. Porfyri, E. Mitsakis, L. Luecken, J. Erdmann, Y. Floetterod, R. Alms, M. Rondinone, and S. Maerivoet. Modelling, Simulation and Assessment of Vehicle Automations and Automated Vehicles' Driver Behaviour in Mixed Traffic. *TransAID Deliverable*, Vol. 3, 2018, p. 1.
30. Lucken, L., E. Mintsis, N. P. Kalliroi, R. Alms, Y.-P. Flotterod, and D. Koutras. From Automated to Manual Modeling Control Transitions With SUMO. Proc., SUMO User Conference, Berlin, Deutschland, 2019.
31. Knoop, V. L., and W. Daamen. Automatic Fitting Procedure for the Fundamental Diagram. *Transportmetrica B: Transport Dynamics*, Vol. 5, No. 2, 2017, pp. 129-144.
32. Liu, H. Generalized Additive Model. Department of Mathematics and Statistics University of Minnesota Duluth, 2008.



33. Maximcsuk, B., Q. Lu, and T. Tettamanti. Determining Maximum Achievable Flows of Autonomous Vehicles Based on Macroscopic Fundamental Diagram. *Perners Contacts*, Vol. 19, No. 2, 2019, pp. 192-199.